Volume 61
Number 59
28 July 2025
Pages 10867–11070

ChemComm

Chemical Communications

rsc.li/chemcomm

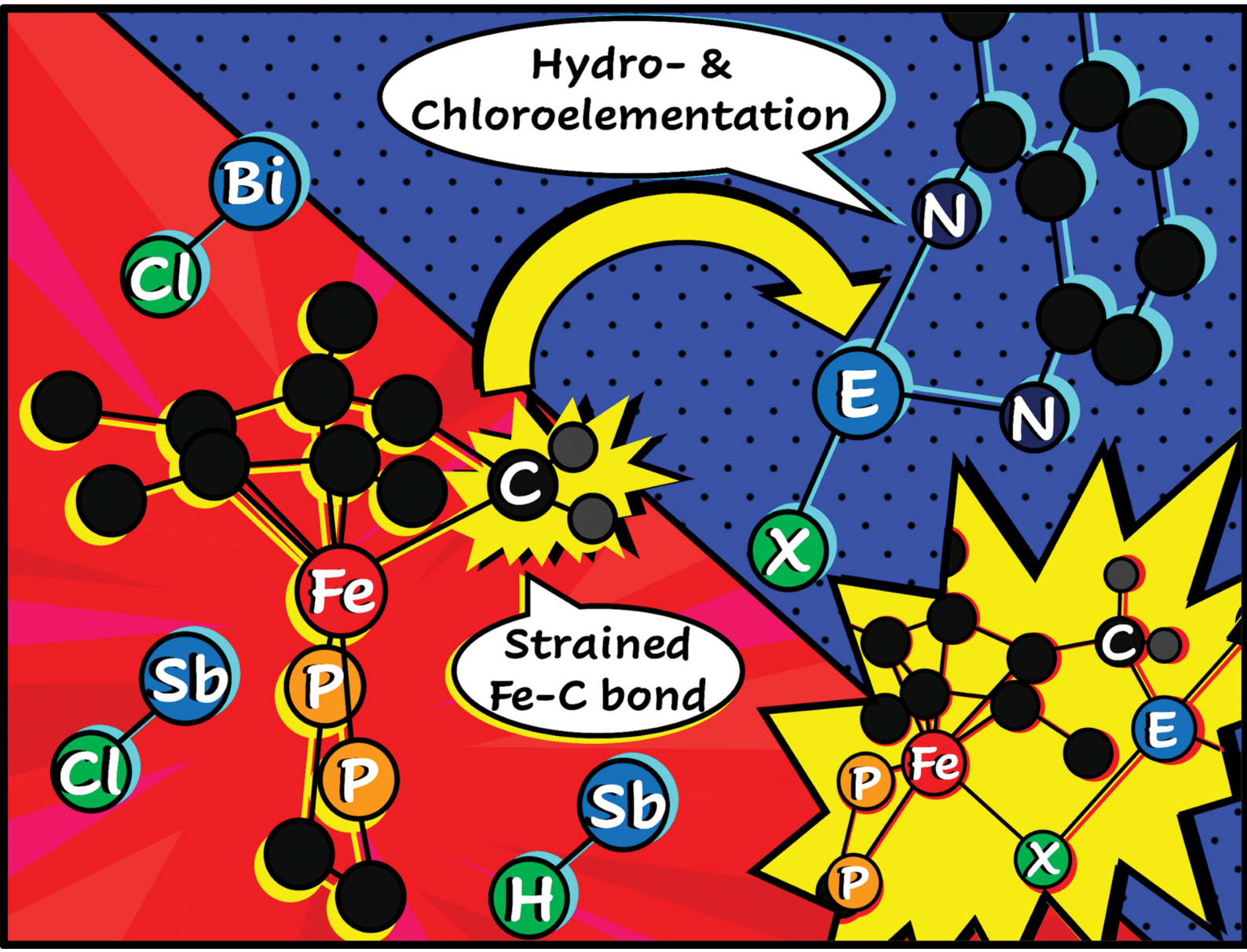

ISSN 1359-7345

ROYAL SOCIETY OF CHEMISTRY

COMMUNICATION

Saurabh S. Chitnis, Marcus W. Drover *et al.*
Hydro- and chloroelementation reactions across an iron–carbon bond using heavy group 15 reagents

ChemComm

COMMUNICATION

View Article Online
View Journal | View Issue

Cite this: *Chem. Commun.*, 2025, **61**, 10969

Received 10th June 2025,
Accepted 24th June 2025

DOI: 10.1039/d5cc03258j

rsc.li/chemcomm

Hydro- and chloroelementation reactions across an iron–carbon bond using heavy group 15 reagents†

Joseph A. Zurakowski,[ab] Mitchell A. Z. MacEachern,[c] Connor S. Durfy,[a] Paul D. Boyle,[a] Saurabh S. Chitnis *[c] and Marcus W. Drover *[a]

Diaminostibines ({Sb}–H) add across the iron–carbon bond of a tucked-in iron diphosphine complex, resulting in hydrostibinated iron hydride [{Cp*-SbR$_2$}Fe–H] complexes. The scope was broadened to include {Sb}–Cl and {Bi}–Cl chloroelementation reactions, providing new and mild synthetic pathways to Sb- and Bi-containing heteroorganometallics.

Hydroelementation is one of the most ubiquitous and useful reactions in synthetic chemistry.[1–4] The addition of an E–H (E = element) bond across an unsaturated unit *e.g.*, the C=C bond of an alkene, serves as a synthetically facile and atom economic strategy to augment molecular complexity in a single step.[5] Both catalytic and stoichiometric E–H (E = B, Al, Si, Ge, Sn, N, P, and S) bond addition processes are known; for many of these, stereo- and enantioselective variants have also been reported.[6–9] Alkene hydroboration, for example, has been well-established as a means to selectively install alcohol functionality following oxidation of an organoborane unit.[10] Moving to Group 14, hydrosilylation (addition of an {Si}–H bond) has led to significant advances in the diversification of organosilicon compounds, which find uses in lubricants, rubbers, and greases.[11,12] Traversing down Group 15, {N}–H (hydroamination) and {P}–H (hydrophosphination) addition reactions have also been developed, providing access to new drug candidates, ligand precursors, and more.[13,14] E–H bond activations featuring heavy Group 15 E–H bonds (E = Sb or Bi) – hydrostibination and hydrobismuthation – are very rare by comparison.[15,16] This is due to both a lack of Lewis-acidic character for Sb (by contrast to commonly employed HBR_2 reagents), and in the case of Bi, a paucity of stable compounds that feature a {Bi}–H bond.[16,17]

Hydrostibination offers access to functionalized {Sb}-containing products, which have shown rich redox chemistry as well as utility as ligands for transition metals, as Lewis-acid additives for catalysis, and for organic synthesis.[18–24] Chitnis and colleagues previously demonstrated the first examples of catalyst- and additive-free hydrostibination of C≡C, C=C, C=O, and N=N bonds (Chart 1A).[15] Ligation of Sb by a rigid naphthalene diamine ligand was key to realizing this reaction, causing the compound's LUMO to resemble a vacant p-orbital, encouraging substrate/{Sb}–H bond interaction. For terminal C≡C bonds, the mechanism of hydrostibination was radical-based, generating the *anti*-addition product.[25] Most other hydroelementation reactions *e.g.*, hydroboration proceed *via* a two-electron pathway, giving a *syn*-addition product; this departure in mechanism and difference

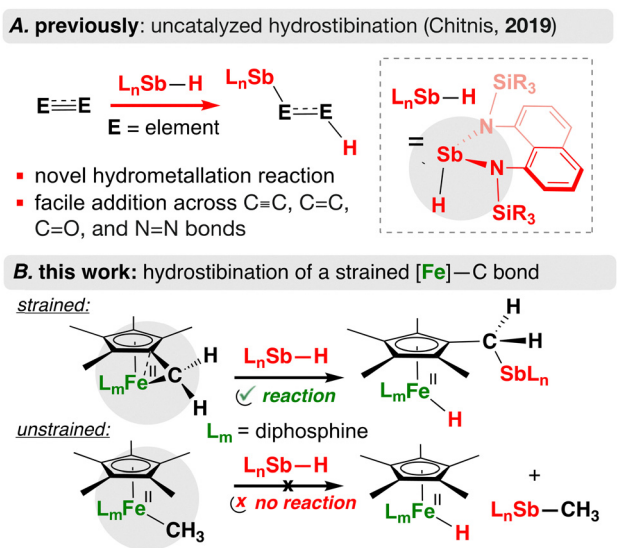

Chart 1 (A) previously: uncatalyzed hydrostibination (Chitnis, 2019); (B) this work: hydrostibination of a strained [Fe]–C bond.

[a] *Department of Chemistry, Western University, 1151 Richmond Street, London, ON, N8K 3G6, Canada. E-mail: marcus.drover@uwo.ca*
[b] *Department of Chemistry and Biochemistry, University of Windsor, 401 Sunset Avenue, Windsor, ON, N9B 3P4, Canada*
[c] *Chemistry Department, Dalhousie University, 6274 Coburg Road, Halifax, Nova Scotia, B3H 4R2, Canada. E-mail: saurabh.chitnis@dal.ca*

† Electronic supplementary information (ESI) available: Spectroscopic data, theoretical calculations, single-crystal X-ray diffraction. CCDC 2450513. For ESI and crystallographic data in CIF or other electronic format see DOI: https://doi.org/10.1039/d5cc03258j

in product profile shapes a need to further develop our understanding of heavy p-block hydroelementation reactions. The scope of {Sb}–H addition reactions has been so far limited to organic substrates. There are no examples where such a functional group has been added across a metal–element bond; such products would represent interesting targets for ligand design, coordination chemistry, cooperative catalysis, and more.[26–29]

Since 2020, the Drover group has examined the role of secondary coordination sphere (SCS) Lewis acids, such as boranes and alanes, on reactivity.[30–34] As an extension, we wondered whether hydrostibination might be used as a tool to introduce an {Sb}-based SCS, providing an entry point towards {M,Sb}-containing compounds. Previously, we reported that a strained Fe tucked-in diphosphine complex[35] underwent hydroboration using $HBCy_2$ to give a {Cp*-BR_2}Fe–H compound. This system was competent for catalytic CO_2 dihydroboration – a reaction sequence that requires an intramolecularly-positioned {Cp*–BR_2} ligand.[33] We now share a collaborative effort that exploits the ring-opening propensity of this strained {Fe}–C complex (Chart 1B)[35] with {Sb}–H, {Sb}–Cl, and {Bi}–Cl reagents, providing the first examples of Fe–carbon, and more generally, metal–element hydro- and chloroelementation reactions[36] using Sb and Bi sources. To our knowledge, related {Sb}–Cl and {Bi}–Cl addition reactions – even with unfunctionalized organic substrates – are unprecedented. By contrast, haloboration has been known since the 1940s.[37]

To begin, treatment of **1**[35] with 1 equiv. of the iso-propylsilyl-substituted 1,8-naphthalene diamine antimony hydride **2a**[15] generated an orange solution of the hydrostibinated Fe(II)-hydride, [(η^5-C_5Me_4-CH_2-{Sb(1,8-Naphth$^{i\text{-Pr}}$)})Fe^{II}(H)(d*n*ppe)] (**3a**; 1,8-Naphth$^{i\text{-Pr}}$ = 1,8-tri(i-propyl)silylamidonaphthalene, d*n*ppe = 1,2-bis(di-*n*-propylphosphino)ethane) (Scheme 1A). This process is characterized by addition of an {Sb}–H unit (δ_H = 9.88 ppm; ν[Sb–H] = 1883 cm^{-1}) across the strained {Fe}–C bond of **1**, generating a ring-opened {Cp*-SbR_2}Fe–H product (δ_H = –18.0 ppm (Fe–H), ν(Fe–H) = 1835 cm^{-1}). Consistent with C_s-symmetry, two resonances are observed for the d*n*ppe *n*-Pr(CH_3) groups at δ_H = 0.95 and 0.89 ppm (forward and backward), as well as two signals at δ_H = 1.92 and 1.86 ppm for the desymmeterized Cp*-ring.

For the Sb fragment, a signal at δ_H = 2.50 ppm is assigned to the {Sb-CH_2Cp*} group, alongside appropriate signals for the coordinated 1,8-naphthalene ligand. By $^{31}P\{^1H\}$ NMR spectroscopy, a singlet at δ_P = 97.0 ppm corresponds to the d*n*ppe ligand. Proving that the [Fe]–H unit in **3a** is derived from the Sb–hydride moiety in **2a**, reaction of **1** with the related Sb–deuteride **2a-d$_1$** produces **3a-d$_1$** (Scheme 1B), defined by a 1 : 1 : 1 triplet at δ_P = 97.0 ppm ($^2J_{P-D}$ = 10.6 Hz) in the $^{31}P\{^1H\}$ NMR spectrum. Given the similarity in NMR and IR spectroscopic features between **3a** and [Cp*Fe^{II}(H)(d*n*ppe)] (δ_H = −17.9 ppm, δ_P = 98.1 ppm, ν(Fe–H) = 1865 cm^{-1}), the peripheral Sb and Fe-bound hydride are non-engaging.[38] Iron(II)-carbon bond hydrostibination was additionally expanded to a triethylsilyl-substituted 1,8-naphthalene diamine antimony hydride **2b**, giving [(η^5-C_5Me_4-CH_2-{Sb(1,8-Naphth^{Et})})-Fe^{II}(H)(d*n*ppe)] (**3b**) (Scheme 1A, see ESI† for details).

Despite our best efforts, compounds **3a**/**b** were not isolable in crystalline form, thwarting analysis by single crystal X-ray diffraction and motivating study by computational means

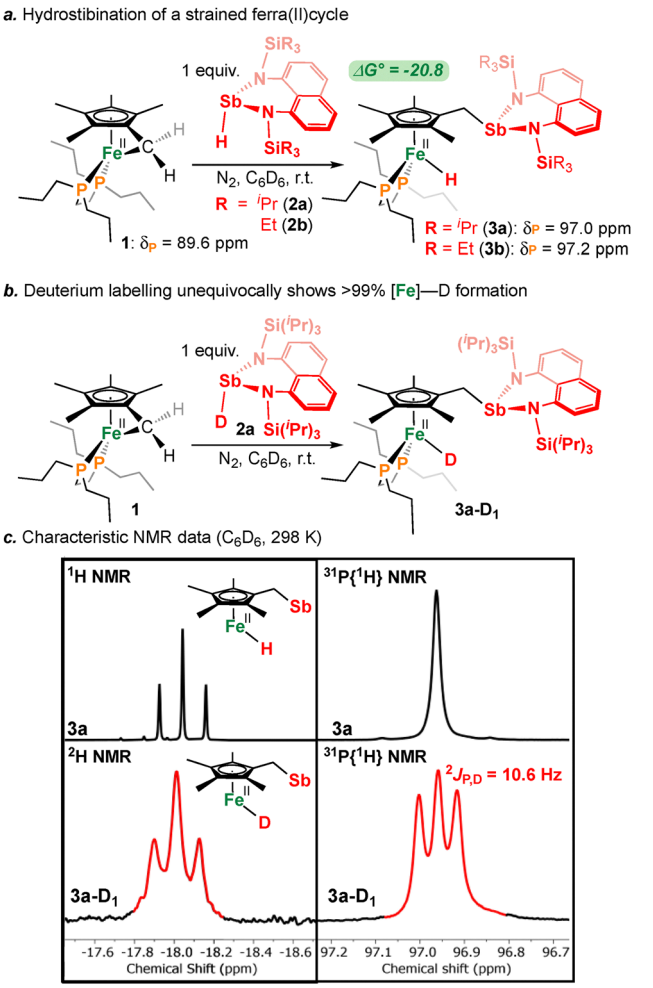

Scheme 1 (A) Hydrostibination of a strained ferra(II)cycle; (B) deuterium labelling unequivocally shows >99% [Fe]–D formation. ΔG° in kcal mol^{-1} calculated at the DLPNO-CCSD(T) level of theory (see ESI† for details); (C) characteristic NMR data (C_6D_6, 298 K).

(Scheme 2). For both **3a**/**b**, the global optimizer algorithm (GOAT)[39–41] within ORCA 6.0.1[42] was used to locate minimum structures. This analysis provided two key geometries that differ by rotation about the Sb–C1 bond, termed 'interacting' where the Sb unit interacts with the Fe-bound hydride (Fe–(μ-H)–Sb) *via* a donor–acceptor interaction, and another, where no such interaction exists ('non-interacting') (Scheme 2). Consistent with spectroscopic observations in solution, DLPNO-CCSD(T)[43–45] calculations reveal an energy difference of 6.1 kcal mol^{-1} (**3a**) and 3.0 kcal mol^{-1} (**3b**) in favour of the non-interacting isomer; the difference between which is attributed to the bulkier –Si(^{i}Pr)$_3$ group in **3a**. For **3b**, this small difference indicates that despite the size of the {Sb(*N*,*N*)} moiety, the system maintains a degree of rotational flexibility. Additional optimizations were carried out for the two halides, (Fe–(μ-X)–Sb) (X = F (**3b-F**) or Cl (**3b-Cl**)), where more favourable interaction energies of 0.4 kcal mol^{-1} (X = Cl) and −3.7 kcal mol^{-1} (X = F) were obtained (see ESI†).

For the μ-H complex, the interacting isomer is characterized by a lengthened {Fe}–H bond of 1.54 Å *cf.*, 1.51 Å for the non-interacting variant; an Sb–H bond length of 2.69 Å is ∼1.0 Å longer than

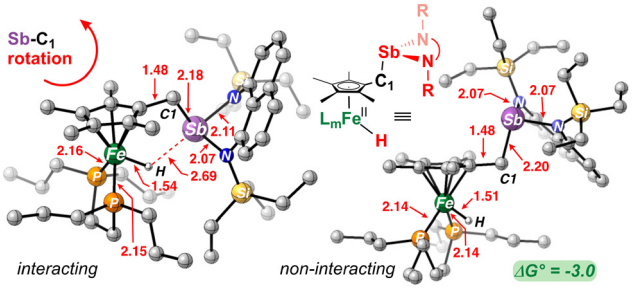

Scheme 2 Probing conformational space about the [Sb]–C bond (**3b**: R = Et). ΔG° in kcal mol^{-1} calculated at the DLPNO-CCSD(T) level of theory (see ESI† for details).

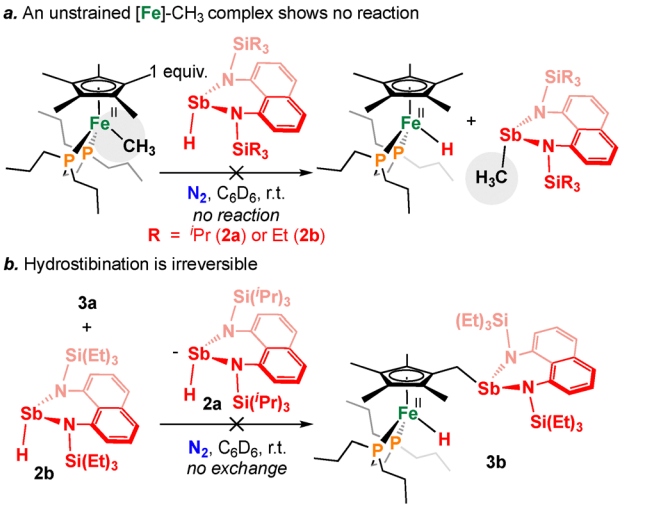

Scheme 3 (A) An unstrained [Fe]–CH_3 model complex shows no reaction with an [Sb]–H; (B) hydrostibination is irreversible.

that noted for free **2b** (1.61(5) Å). This interaction, which results in some degree of [{Fe}–H] → [{Sb}–N](σ*) donation, prompts slight lengthening of the *trans*-Sb–N bond (2.11 Å) *cf.*, 2.07 Å for the non-interacting isomer and an average length of 2.05 Å seen in the crystal structure of **2b** (Scheme 2).[15] Thermodynamic calculations additionally revealed that hydrostibination of **1** is exergonic for both {Sb}–H compounds: $\Delta G^{\circ} = -20.8$ kcal mol^{-1} for both **3a** and **3b** (Scheme 1A).

To our knowledge, complexes **3** represent the first example of hydrostibination across a metal–element bond, giving access to the only known {Cp*-SbR_2} compounds. Seeking to expose whether a strained unit is requisite for reaction success, the iso-propyl- and ethyl-substituted antimony hydrides **2a/b** were combined with the acyclic model complex, [Cp*Fe(d*n*ppe)(CH_3)],[38] which contains an {Fe}–CH_3 bond (Scheme 3A). Combination of these reagents, however, resulted in null reactivity – hydride transfer was not observed. This outcome speaks to the role of **1** as a substrate for the introduction of a secondary Sb unit *via* hydrostibination.

For some E–H hydroelementation reactions, retro- or dehydroelementation (the reverse) is known to readily occur.[46–48] The reversibility of hydrostibination was accordingly probed using a cross-over experiment between **3a** and **2b**, though this reaction did not result in exchange; formation of **3b** and **2a** was not witnessed (Scheme 3B). Further cementing lack of {Sb} dissociation, compounds **3a/b** do not dissociate in the presence of aldehydes *e.g.*, benzaldehyde – a known hydrostibination substrate for compounds **2**.[15] Together, these experiments suggest that once reacted, Sb becomes irreversibly attached to the {Cp*Fe} organometallic fragment and indicates that the Sb–H bond in **2a/b** is not sufficiently basic to deprotonate the methyl group of the Cp* ligand of [Cp*Fe(d*n*ppe)(CH_3)].

Heavy-atom addition was also expanded to include chlorostibination and -bismuthation. While scrambling of groups between EAr_3 and Ar_2ECl compounds is known to yield $ArECl_2$ derivatives,[49] the elementary chlorometallation step underlying in these reactions has not been exploited in an additive fashion to access structures of greater complexity. To this end, combination of **1** with 1 equiv. of the related diamino {Sb}–Cl (**4a**) or {Bi}–Cl (**4b**) reagent led to ring-opening, providing the {Fe}–Cl complex having an appended {Sb} (**5a**, δ_P = 78.0 ppm) or {Bi} (**5b**, δ_P = 78.3 ppm) unit (Scheme 4A); these $^{31}P\{^1H\}$ NMR data are similar to unfunctionalized [Cp*Fe(d*n*ppe)(Cl)] (δ_P = 79.4 ppm).[38] Gratifyingly, complex **5b** was amenable to analysis by single-crystal X-ray diffraction, revealing a bridging μ-Fe–Cl–Bi unit (d_{Bi-Cl} = 2.9944(13) Å) (Scheme 4B) with an Fe–Cl bond length (d_{Fe-Cl} = 2.339(1) Å) similar to unfunctionalized [Cp*Fe(d*n*ppe)(Cl)] (2.349(1) Å).[38] For Bi, thermodynamic calculations of compounds (Fe–(μ-X)–Bi) (X = H, F or Cl (**5b**)) revealed similarity in both magnitude and trend to the Sb analogues discussed above, with more favourable interactions being made across the series: 1.6 kcal mol^{-1} (X = H), −1.6 kcal mol^{-1} (X = Cl), and −6.5 kcal mol^{-1} (X = F) (see ESI† for details).

Lewis acids are increasingly recognized for their role in iron-mediated N_2 fixation, particularly in systems where cooperative substrate binding facilitates activation and reduction to [Fe]–N_xH_y products.[50,51] To explore a model for such cooperative interactions using a heavy Group 15 element, {Fe,E} (E = Sb, Bi) cations were computationally modelled using hydrazine as a substrate (Scheme 4C). These studies reveal that the μ-NH_2NH_2 bridging mode is thermodynamically favoured by 0.7 and 2.3 kcal mol^{-1} for both Sb and Bi, indicating feasibility of cooperative engagement. The optimized structures show Sb-N (2.7814 Å) or Bi-N (2.8223 Å) contacts involving the μ-NH_2NH_2 unit that are significantly shorter than the sum of their respective van der Waals radii (Sb–N: 3.61 Å, Bi–N: 3.62 Å).[52] Importantly, this binding event results in a significant acidification of the N_β–H proton—by 14–17 pK_a units—underscoring the ability of such heavier Group 15 elements to modulate substrate properties. Consistent with increased [{Sb}–N](σ*) donation, a decrease in E–N_2H_y bond distance correlates with an increase in E–N(*trans*) bond length (graph, Scheme 4C). This work provides, to our knowledge, the first conceptual framework for employing heavy Group 15 Lewis acids in such a role.[53]

Herein, we have disclosed the first example of hydro- and chloroelementation reactions across a metal–carbon bond using heavy Group 15 compounds, which occurs under ambient conditions in near-quantitative fashion (by ^{31}P NMR spectroscopy). The success of this reaction depends on the strained nature of the Fe diphosphine tucked-in complex **1**, as exemplified by null reactivity with an unstrained [Fe]–CH_3 model complex. These findings

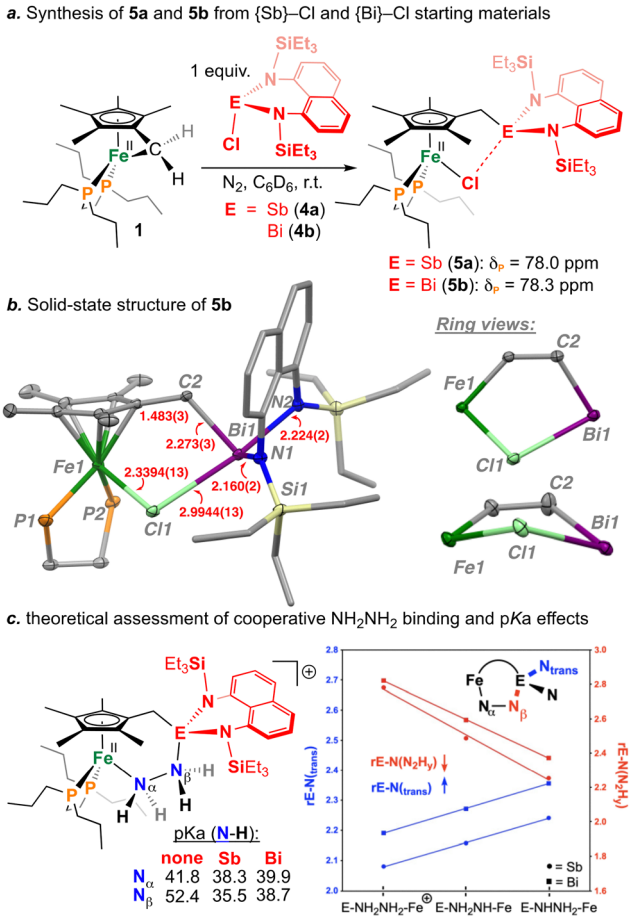

Scheme 4 (A) Synthesis of **5a** and **5b** from chloride starting materials; (B) solid-state structure of **5b** with an enhanced view of the [Fe]–Cl–{Bi} interaction (ellipsoids drawn at 50% probability; hydrogen atoms and dnppe ^{n}Pr groups have been omitted for clarity); (C) theoretical assessment of cooperative NH_2NH_2 binding and pK_a effects.

represent an advance in main group–transition metal reactivity because they offer new and mild avenues (compared to salt metathesis or dehydrohalogenation) for designing cooperative heterobimetallic systems involving heavy p-block elements.[54]

J. A. Z. performed all experimental work using complex **1** and performed all computations. M. M. prepared all Sb- and Bi-containing reagents **2a**, **2a-D$_1$**, **2b**, **4a**, and **4b**. M. W. D. and S. S. C. supervised the project. C. S. D. performed the first reaction between **1** and **2a-D$_1$** and discovered the hydrostibination reaction. J. A. Z. collected the solid-state data for **5b**, and it was solved/refined by P. D. B. All authors were involved in writing, reviewing, and editing drafts of the paper.

M. W. D. is grateful to Western University, the Council of Ontario Universities for a John C. Polanyi award, the Canadian Foundation for Innovation (LOF-212442), and NSERC (Discovery Grant, RGPIN-2020-04480, Discovery Launch Supplement, DGECR-2020-00183), and graduate award (CGS-D/NSERC Vanier to J. A. Z.) for funding. S. S. C. is grateful to Dalhousie University, the Alfred P. Sloan Research Fellowship, and NSERC (RGPIN-2024-04790) for funding. We acknowledge Tamina Z. Kirsch for obtaining elemental analysis data.

Conflicts of interest

There are no conflicts to declare.

Data availability

The data supporting this article have been included as part of the ESI.† Crystallographic data for **5b** has been deposited at the CCDC under 2450513.

References

1 M. Wathier and J. A. Love, *Eur. J. Inorg. Chem.*, 2016, 2391–2402.
2 S.-L. Shi and S. L. Buchwald, *Nat. Chem.*, 2015, **7**, 38–44.
3 G. Chakraborty and S. Maity, *Adv. Synth. Catal.*, 2025, **367**, e202401239.
4 S. Park, *ChemCatChem*, 2024, **16**, e202301422.
5 J. V. Obligacion and P. J. Chirik, *Nat. Rev. Chem.*, 2018, **2**, 15–34.
6 F. Gao and A. H. Hoveyda, *J. Am. Chem. Soc.*, 2010, **132**, 10961–10963.
7 X.-H. Yang, *et al.*, *J. Am. Chem. Soc.*, 2019, **141**, 3006–3013.
8 M. R. Radzhabov and N. P. Mankad, *Org. Lett.*, 2021, **23**, 3221–3226.
9 L.-J. Cheng and N. P. Mankad, *J. Am. Chem. Soc.*, 2019, **141**, 3710–3716.
10 H. C. Brown and G. Zweifel, *J. Am. Chem. Soc.*, 1959, **81**, 247.
11 J.-L. Panayides, *et al.*, *RSC Med. Chem*, 2024, **15**, 3286–3344.
12 L. D. De Almeida, *et al.*, *Angew. Chem., Int. Ed.*, 2021, **60**, 550–565.
13 T. Shima, *et al.*, *Nature*, 2024, **632**, 307–312.
14 L. Rosenberg, *ACS Catal.*, 2013, **3**, 2845–2855.
15 K. M. Marczenko, *et al.*, *Angew. Chem., Int. Ed.*, 2019, **58**, 18096–18101.
16 K. L. Mears, *et al.*, *J. Am. Chem. Soc.*, 2024, **146**, 19–23.
17 P. Novák, *et al.*, *Dalton Trans.*, 2023, **52**, 218–227.
18 Y. Huang, *et al.*, *Tetrahydron Lett.*, 1985, **26**, 5171–5172.
19 H. J. Breunig and J. Probst, *J. Organomet. Chem.*, 1998, **571**, 297–303.
20 J. S. Jones and F. P. Gabbaï, *Acc. Chem. Res.*, 2016, **49**, 857–867.
21 N. R. Champness and W. Levason, *Coord. Chem. Rev.*, 1994, **133**, 115–217.
22 A. P. M. Robertson, *et al.*, *Angew. Chem., Int. Ed.*, 2014, **53**, 6050–6069.
23 L. Wu, *et al.*, *ACS Org. Inorg. Au*, 2025, **5**, 13–25.
24 C. Jones, *Coord. Chem. Rev.*, 2001, **215**, 151–169.
25 J. W. M. MacMillan, *et al.*, *Chem. – Eur. J.*, 2020, **26**, 17134–17142.
26 V. A. Béland and P. J. Ragogna, *Chem. – Eur. J.*, 2020, **26**, 12751–12757.
27 A. W. Knights, *et al.*, *Chem. Sci.*, 2019, **10**, 7281–7289.
28 A. M. Priegert, *et al.*, *Chem. Soc. Rev.*, 2016, **45**, 922–953.
29 D. G. Brown and J. Boström, *J. Med. Chem.*, 2016, **59**, 4443–4458.
30 A. D. Dilinaer, *et al.*, *Dalton Trans.*, 2024, **53**, 13298–13307.
31 G. J. Jobin, *et al.*, *Organometallics*, 2025, **44**, 148–157.
32 M. W. Drover, *Chem. Soc. Rev.*, 2022, **51**, 1861–1880.
33 C. S. Durfy, *et al.*, *Angew. Chem., Int. Ed.*, 2025, **64**, e202421599.
34 J. A. Zurakowski, *et al.*, *Trends Chem.*, 2022, **4**, 331–346.
35 J. A. Zurakowski and M. W. Drover, *Chem. Commun.*, 2023, **59**, 11349–11352.
36 Use of the term 'hydroelementation' is consistent with related work that describes E–H bond addition reactions across strained rings *e.g.*, of cyclopropanes and epoxides. See (*a*) M. Murai, *et al.*, *Chem. Commun.*, 2017, **53**, 9281–9284; (*b*) H. Kondo, *et al.*, *J. Am. Chem. Soc.*, 2020, **142**, 11306–11313; (*c*) D. Wang, *et al.*, *Angew. Chem., Int. Ed.*, 2018, **57**, 16861–16865; (*d*) M. Magre, *et al.*, *J. Am. Chem. Soc.*, 2020, **142**, 14286–14294.
37 S. Kirschner, *et al.*, *New J. Chem.*, 2021, **45**, 14855–14868.
38 J. A. Zurakowski, *et al.*, *Inorg. Chem.*, 2023, **62**, 7053–7060.
39 D. J. Wales and J. P. K. Doye, *J. Phys. Chem. A*, 1997, **101**, 5111–5116.
40 C. Bannwarth, *et al.*, *J. Chem. Theory Comput.*, 2019, **15**, 1652–1671.
41 S. Goedecker, *J. Chem. Phys.*, 2004, **120**, 9911–9917.
42 F. Neese, *WIREs Comput. Mol. Sci.*, 2022, **12**, e1606.
43 C. Riplinger and F. Neese, *J. Chem. Phys.*, 2013, **138**, 034106.
44 C. Riplinger, *et al.*, *J. Chem. Phys.*, 2013, **139**, 134101.
45 C. Riplinger, *et al.*, *J. Chem. Phys.*, 2016, **144**, 024109.
46 K.-W. Chiu and E.-I. Negishi, *J. Organomet. Chem.*, 1976, **112**, C3–C6.
47 N. M. Weliange, *et al.*, *Organometallics*, 2014, **33**, 4251–4259.
48 J. C. Hilario-Martínez, *et al.*, *Chem. Sci.*, 2020, **11**, 12764–12768.
49 M. Wieber, *et al.*, *Z. Anorg. Allg. Chem.*, 1983, **505**, 134–137.
50 J. J. Kiernicki, *et al.*, *Chem. Sci.*, 2019, **10**, 5539–5545.
51 J. B. Geri, *et al.*, *J. Am. Chem. Soc.*, 2017, **139**, 5952–5956.
52 M. Mantina, *et al.*, *J. Phys. Chem.*, 2009, **113**, 5806–5812.
53 For a report using BR_3, see J. J. Kiernicki, *et al.*, *Chem. Commun.*, 2020, **56**, 13105–13108.
54 V. K. Greenacre, *et al.*, *Coord. Chem. Rev.*, 2021, **432**, 213698.